Localization in random electron systems: Al$_x$Ga$_{1-x}$As alloys and intentionally disordered GaAs/Al$_x$Ga$_{1-x}$As superlattices

Yu. A. Pusep[1] and A. Rodriguez[2]

[1]*Instituto de Fisica de São Carlos, Universidade de São Paulo, 13460-970 São Carlos, São Paulo, Brazil*
[2]*Departamento de Fisica Fundamental, Universidad de Salamanca, 37008 Salamanca, Spain*

The localization properties of single-particle and collective excitations were investigated in Al$_x$Ga$_{1-x}$As alloys and in intentionally disordered GaAs/Al$_x$Ga$_{1-x}$As superlattices by magnetoresistance and Raman scattering. It is shown that the Landau damping determines the localization length of the collective plasmonlike excitations in bulk Al$_x$Ga$_{1-x}$As alloy, while the electrons are localized due to the alloy random potential. Meanwhile, the localization lengths of both the single-particle and collective excitations are limited by disorder in the intentionally disordered superlattices. In such a case, a comparison between the localization properties of the single-particle and collective excitations propagated in the same random potential is possible. The localization length of the individual electron is found to be considerably larger than the localization length of their collective excitations. This implies that the electron-electron interaction which is fundamental for the collective excitations increases localization. However, the difference between the localization of the single-particle and collective excitations decreases with the increasing disorder. Consequently, in clean electron systems the effect of the interaction on localization of elementary excitations is stronger. Additionally, a reasonable agreement has been found between the measured localization lengths for the single particle in the disordered superlattices and those numerically obtained from transfer matrix calculations.

I. INTRODUCTION

The question of how localization of electrons in disordered systems is affected by the interaction between them has attracted continued interest for many decades. Today, it is known that the comparatively simple models developed for noninteracting electrons are insufficient for understanding the accumulated experimental data.[1] One of the most intriguing yet unsolved problem is linked to the metal-to-insulator transition found in two-dimensional electron systems.[2] A possible explanation of this problem is linked to the electron-electron interaction.[3,4] However, until now there is no definite agreement how the interaction influences localization. It is believed that weak interaction reduces localization, while strong interaction increases it.[5,6] Although in some aspects two-dimensional electrons behave in a way very different from the three-dimensional case, however, in general the interaction between free electrons results in collectivization of elementary excitations, independent of dimensionality. Therefore, investigation of the effects of the interaction in three-dimensional systems can shed some light on common properties of interacting disordered electron systems. One could imagine the following experiment which may explain how the interaction influences localization: measuring the conductivity of a disordered electron system with a key which controls the interaction. Then, the comparison between the localization length measured in a disordered electron system without interaction and that with interaction will reveal the role of the interaction. Such experiments were performed in two-dimensional electron systems where the gate voltage controls the electron density, thus switching the system between weak and strong interaction limits. On the other hand, variations of the gate voltage and the electron density significantly influence electron scattering and screening effects which also contribute to the conductivity.[7] This complicates the analysis of experimental data in two-dimensional systems. Another method to examine the influence of the interaction on localization of electrons was presented in our recent publication.[8] In this work, we compared the localization lengths of the single-particle and collective electron excitations (plasmons) in disordered electron systems created by the random potential of intentionally disordered semiconductor superlattices (SLs). The SLs were grown to produce a Gaussian-type energy disorder, characterized by a controlled strength parameter. This type of disorder, apart from being the most general disorder appearing in natural disordered systems, also allows a direct comparison of the experimental data with the existing localization theories. The intentionally disordered SLs were firstly proposed in the celebrated work of Esaki and Tsu.[9] Later in such SLs the electron localization was demonstrated.[10] The most important consecutive works studying SLs with artificial disorder are listed in Ref. 11.

In the case of high electron density, the Fermi liquid theory determines a one-to-one correspondence between the transport properties of the low-energy single-particle excitations and the noninteracting electrons, while Coulomb interaction intrinsically determines properties of the plasmons. Therefore, a difference between the localization lengths of the electrons and the plasmons can be naturally assigned to the effect of the interaction.

In the above cited article,[8] we demonstrated that the electron localization length is considerably longer than that of the plasmons, which implies that the electron-electron interaction increases localization. The data were obtained in three samples. In this work, we present additional evidences of this effect. We measured the localization lengths of the electrons and their collective excitations in a variety of samples in

different disordered electron systems such as $Al_xGa_{1-x}As$ alloys and $GaAs/Al_xGa_{1-x}As$ intentionally disordered SLs. In the alloys the disorder was provided by the alloy potential fluctuations, while in the SLs the vertical (along the growth direction) disorder was produced by a controlled random variation of the well thicknesses. In both cases, the localization lengths of the electrons were found to be significantly longer than those of the plasmons. Furthermore, we demonstrated a crucial role of the Landau damping which usually limits the localization length of the collective electron excitations in strongly disordered three-dimensional electron systems (alloys). However, at certain conditions the Landau damping is absent in the SLs; therefore, the disorder determines the localization of both the plasmons and the electrons inside these systems.

The paper is organized as follows. The sample structures and the experimental routines are shown in Sec. II. Theoretical considerations are given in Sec. III. Experimental data and their analyses obtained in the $Al_xGa_{1-x}As$ alloys and in the disordered $GaAs/Al_xGa_{1-x}As$ SLs are presented in Secs. IV and V, respectively, while conclusions are outlined in Sec. VI.

II. EXPERIMENT

Differently doped 0.5 μm thick $Al_{0.11}Ga_{0.89}As$ films were grown by molecular beam epitaxy on semi-insulating (001) GaAs substrates. Lowly and highly doped alloys demonstrated insulating and metallic behavior, respectively. A crossover between transport regimes occurred at the electron concentration $n=5 \times 10^{17}$ cm^{-3}. Mobilities of the metallic alloys were found in the interval 1100–1500 cm^2/V s. Furthermore, 50 periods of the intentionally disordered $(GaAs)_m(Al_{0.3}Ga_{0.7}As)_6$ SLs [where the thicknesses of the layers are expressed in monolayers (ML)] with various strengths of the disorder were grown on semi-insulating and doped (001) GaAs substrates. In order to decrease the influence of the interface roughness, the growth was interrupted for 30 s at each interface. In this case, the disorder was produced by a controlled random variation of the well thicknesses (m) around the nominal value of 17 ML. The disorder strength was characterized by the disorder parameter δ_{SL} introduced in the next section. Such a disorder let us control the spatial extent of the wave functions of the elementary excitations propagating normal to the layers. In order to form the degenerate electron system, the SLs were homogeneously doped with Si.

The Raman backscattering was used to measure the localization lengths of the collective plasmon–LO-phonon excitations propagated perpendicular to the surface of the samples. The Raman scattering was collected at $T=10$ K by an Instruments S.A. T64000 triple grating spectrometer supplied with a charge coupled device detector cooled by liquid nitrogen; the 5145 Å line of an Ar$^+$ laser was used for nonresonant excitation.

Because of the isotropy of the alloys, there was no need to measure the localization properties of the electrons propagated in the same direction as the plasmons. Therefore, in this case the magnetotransport experiments parallel to the sample surface were carried out by the standard four-probe method using Hall bar structures. The disordered SLs grown on doped substrates were used for the vertical magnetotransport measurements in order to determine the localization lengths of the electrons propagated in the same direction (perpendicular to the layers) as the plasmons. These measurements were realized in the square shaped-double-mesa structures with areas of 1×1 mm^2 described in Ref. 8. Magnetotransport measurements parallel to the layers were realized in the identical SLs grown on semi-insulating substrates. The Hall bar structures used for the parallel magnetotransport measurements in alloys and SLs had active areas of 550×200 μm^2. Both the Hall bar and mesa structures were produced by low-rate chemical etching. The Ohmic contacts were fabricated by depositing either In (Hall bars) or a Au:Ge:Ni alloy (mesas). The transport measurements were performed with the current of 10^{-5}–10^{-4} Å by standard low-frequency (1 Hz) lock-in technique using the Perkin Elmer Instruments amplifier, Model 7280 DSP, in a pumped liquid He cryostat in magnetic fields directed perpendicular to the current in the temperature range from 1.6 to 15 K.

III. THEORETICAL CONSIDERATIONS

As in Ref. 8, the electron phase-breaking length determined by the magnetoresistance measurements was used to estimate the localization length of the single-particle electron excitations. In the weak-localization regime ($k_F l \gg 1$, where k_F and l are the Fermi wave number and the elastic free path length, respectively) and in a weak magnetic field ($\omega_c \tau \ll 1$, where ω_c and τ are the cyclotron frequency and the elastic scattering time, respectively), the magnetic field dependence of the conductivity is caused by the weak-localization correction. In the magnetic field $H_\perp$ orthogonal to the plane of the layers, the weak-localization corrections to the parallel conductivity of a SL are determined by the following expression:[12]

$$\Delta\sigma^{\parallel}(H) = \frac{e^2}{2\pi^2\hbar l_H}\alpha F(\delta), \tag{1}$$

where $l_H = \sqrt{\hbar/eH_\perp}$ is the magnetic length, $\alpha = \sqrt{m_z/m_\parallel}$ is the coefficient of anisotropy, $F(\delta)$ is the Kawabata function,[13] and $\delta = \frac{l_H^2}{4L_\varphi^2}$ with L_φ being the electron phase coherency length. This is just the anisotropic form of the quantum correction obtained in Ref. 13 in the three-dimensional isotropic case (when $\alpha=1$). As it was shown in Ref. 14, the quantum correction to the vertical (perpendicular to the surface) magnetoconductivity of a SL measured in the magnetic field perpendicular to the layers is determined by the anisotropic formula (1) divided by α^2, while the conductivity correction in the magnetic field parallel to the layers can be obtained by scaling the field according to the scaling relation $H_\parallel = H_\perp/\alpha$. Thus, a fit of the experimental magnetoresistance data provides for a value of the electron coherency length, which in our case is associated with the electron localization length.

Quantitative control of the disorder strength in the intentionally disordered SLs allowed a direct comparison of the experimentally obtained localization lengths with those cal-

culated numerically. The localization lengths of the single-particle excitations have been numerically studied using the transfer matrix technique, in different realizations of the disordered superlattices for a given value of the disorder parameter. The SLs have been modeled by a one-dimensional Kronig-Penney potential with variable effective mass. The relevant parameters used for the simulations are as follows: barrier width $L_b=6$ ML, band offset $V=300$ meV, effective mass in barriers $m_b=0.092m_0$, and effective mass in wells $m_w=0.067m_0$. The different widths of the wells vary around the nominal value $L_w=17$ ML, and the value for the monolayer width was set to 3.0 Å. As described in the previous section, disorder is included in the system by a fluctuation of the well thickness, according to a probability distribution which is obtained from a Gaussian probability density for the electron energy in the isolated well. The Gaussian is centered at the value of the energy E_0 corresponding to the 17 ML well and it is characterized by its full width at half maximum Δ. From the Gaussian density, the probability distribution for the well thickness L_w can be easily constructed, and it is characterized by the parameter $\delta_{SL}=\Delta/W$, where W is the miniband width of the ordered SL. Using the parameters given above, we obtained $E_0=79.92$ meV and $W=52.39$ meV. Once a finite disordered SL is generated for a given value of δ_{SL}, the transfer matrix formalism is used to obtain the transmission probability of the structure as a function of the energy $T(E)$. From this quantity, the electronic localization can be characterized by the Lyapunov exponent defined as $\lambda(E)=-(2L)^{-1}\ln T(E)$, where L is the length of the system. For every energy, the electronic localization length is determined by $1/\lambda(E)$. The transmittance of the disordered SL is then characterized by the transmission efficiency T_{eff}, which corresponds to the area enclosed by $T(E)$ per energy unit,

$$T_{\text{eff}} = \frac{1}{\Delta E}\int_{E_F-\Delta E}^{E_F} T(E)dE, \tag{2}$$

where the integration is carried out over all the occupied states below the Fermi energy, which in all cases is considered to be $E_F=90$ meV (corresponding to the doping of the SLs used for vertical magnetotransport measurements). The sample can then be characterized by an effective localization length for the electrons defined as $L_z=-2L/\ln T_{\text{eff}}$.

A theory establishes direct correspondence between the intensity of Raman scattering and the plasmon wave function.[15] Therefore, Raman scattering presents the perfect tool to study the influence of the disorder on localization of the collective electron excitations. In the recent article,[16] we have shown that in the intentionally disordered GaAs/Al$_x$Ga$_{1-x}$As SLs the observed asymmetry of the Raman lines assigned to the plasmonlike collective excitations is due to the effect of their localization. In the presence of disorder, the plasmons can be represented as a superposition of plane waves with the wave vectors distributed in a finite interval Δq, which gives rise to their finite spatial extent—the localization length L_p. This implies that, contrary to the perfect crystal, where the collective excitations with a wave number q_0 contribute to Raman scattering, in the disordered

systems all the modes in the interval of the wave number uncertainty $\Delta q \simeq \pi/L_p$ determine the Raman intensity. At a small enough localization length, the interval of the relevant wave numbers may cover the region of the significant dispersion and then an asymmetrical shape of the Raman line emerges. In this case, the magnitude of the localization length of the collective excitations indicates the strength of the correlation effects: the longer the localization length, the stronger the electron correlation. The intensity of the relevant Raman line is given by[16]

$$I(\omega) \sim \int \exp\left[-\frac{(q-q_0)^2 L_p^2}{4}\right]\frac{d^3q}{[\omega-\omega_p(q)]^2+(\Gamma/2)^2}, \tag{3}$$

where $q_0=4\pi n(\lambda)/\lambda$ is the wave number of the laser light with the wavelength λ used for excitation, $n(\lambda)$ is the refractive index, $\omega_p(q)$ is the dispersion of the appropriate collective excitations, and Γ is their damping constant.

The dispersions of the collective modes were calculated in the random phase approximation (RPA) as in Ref. 16. In the absence of strong localization, the structural disorder does not considerably affect the plasmon dispersion which is due to the interaction between free electrons. In the absence of the Landau damping, the validity of the RPA was confirmed in Ref. 17.

IV. LOCALIZATION IN Al$_x$Ga$_{1-x}$As ALLOY

The influence of disorder on dynamic electron properties depends on the relation between the disorder energy (Δ) and the Fermi energy (E_F). The disorder energy of Al$_x$Ga$_{1-x}$As alloy (alloy potential), which is determined by a difference between atomic potentials of cations is fixed and equals to $\Delta_{alloy}=0.2$ eV.[18] Thus, the metal ($E_F>\Delta$) and insulating ($E_F<\Delta$) transport regimes can be realized in the Al$_x$Ga$_{1-x}$As alloy when changing doping concentration. Both of these regimes achieved in differently doped Al$_x$Ga$_{1-x}$As alloys manifest themselves in the temperature dependences of the resistivities depicted in Fig. 1. The variation of the resistivity with the temperature obtained in the lowly doped Al$_x$Ga$_{1-x}$As is well explained by the variable-range hopping mechanism:[19]

$$\rho(T) = \rho_0 \exp\left[\left(\frac{T_0}{T}\right)^{1/4}\right]. \tag{4}$$

The best fitting of the calculated resistivity to the experimental data was obtained with the characteristic temperature $T_0=341$ K, corresponding to the disorder energy $\Delta=0.29$ eV, which is in reasonable agreement with the alloy potential known in Al$_x$Ga$_{1-x}$As alloy (mentioned above). The weak temperature variation of the resistivity observed in the metallic Al$_x$Ga$_{1-x}$As is caused by the temperature destruction of the quantum interference. We found this variation to be proportional to $T^{-3/2}$, which corresponds to the electron-phonon inelastic scattering.[20]

The magnetoresistance data obtained in metallic and insulating Al$_x$Ga$_{1-x}$As are shown in Fig. 2. The different concavi-
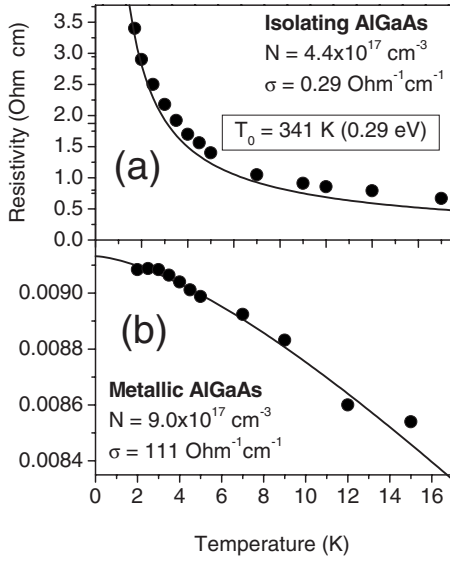
FIG. 1. Temperature dependences of the zero-field resistivities measured in the (a) insulating and (b) metallic $Al_{0.11}Ga_{0.89}As$ alloys. The full lines in panels (a) and (b) represent the calculated variable-range hopping resistivity and the resistivity due to the quantum interference effects, respectively.

ties, a positive one in the metallic regime and a negative one in the insulating regime, were found in excellent agreement with the results obtained recently in the disordered SLs in Ref. 21, where the modification of the magnetoresistance during the metal-to-insulator transition was studied. The fits made in the alloys in the same ways as in the disordered SLs [using the isotropic form of formula (1)] provide the electron coherence lengths L_φ in the corresponding regimes. They are shown for different temperatures in Fig. 3. The T^{-2} dependence corresponding to the dephasing in an ideal Fermi liquid[22] describes well the temperature behavior of the coherence length in the metallic alloy. Similar to the disordered SLs, a much weaker temperature dependence of the coherence length was observed in the insulating regime as compared to that in the metallic one.
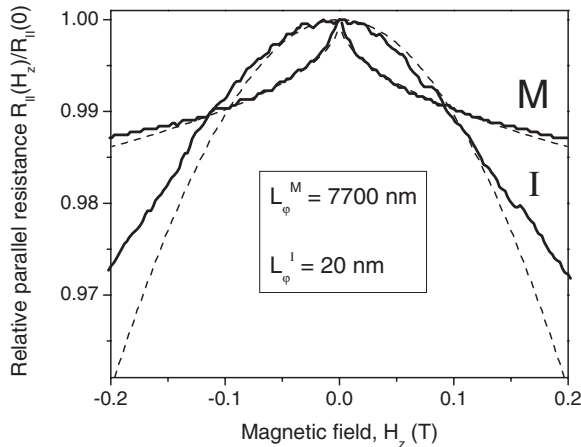

FIG. 2. Relative magnetoresistivities measured at $T=1.6$ K in the metallic (M) and insulating (I) transport regimes in $Al_{0.11}Ga_{0.89}As$ alloys with $n=9.0\times10^{17}$ cm^{-3} and $n=4.4\times10^{17}$ cm^{-3}, respectively.
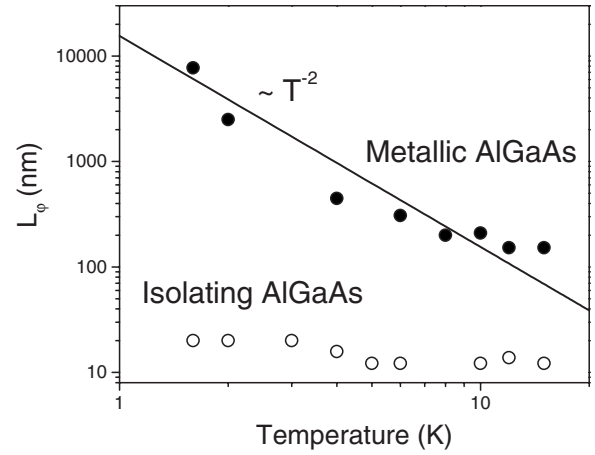

FIG. 3. Temperature dependences of the coherence lengths L_φ obtained in the metallic (closed circles) and insulating (open circles) $Al_{0.11}Ga_{0.89}As$ alloys with $n=9.0\times10^{17}$ cm^{-3} and $n=4.4\times10^{17}$ cm^{-3}, respectively. The full line is the dependence calculated according to T^{-2}.

The localization of the AlAs-like plasmon-phonon collective excitations was already studied in $Al_xGa_{1-x}As$ alloys in Ref. 23. The data shown in Fig. 4 represent the localization lengths of these plasmonlike excitations obtained by Raman scattering in $Al_xGa_{1-x}As$ alloys as a function of the doping concentration. At low doping, the electrons are localized by the random alloy potential. A typical temperature behavior of the resistivity shown for one of these isolating alloys in Fig. 1(a) confirms the localization. In this case, the relevant Raman lines revealed asymmetries characteristic of the LO phonons, and consequently, the obtained localization length corresponds to the spatial localization of the optical lattice
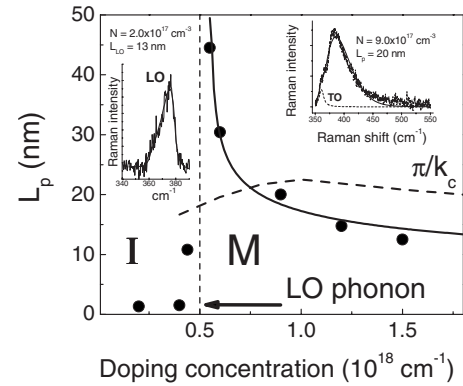

FIG. 4. Localization lengths of the AlAs-like plasmon–LO-phonon collective excitations measured in differently doped insulating (I) and metallic (M) $Al_{0.11}Ga_{0.89}As$ alloys at $T=10$ K. The full line exhibits the decrease of the plasmon localization length caused by the interaction of the plasmons with the ionized impurities (Ref. 23). The dash line shows the dependence of the inverse characteristic wave number π/k_c on the electron concentration. Typical Raman lines due to the AlAs-like LO phonons and the coupled mode in the insulating and metallic alloys, respectively, are shown in the corresponding insets together with the fitting data. A weak contribution caused by the forbidden LO phonons is seen in the heavily doped metallic alloy.
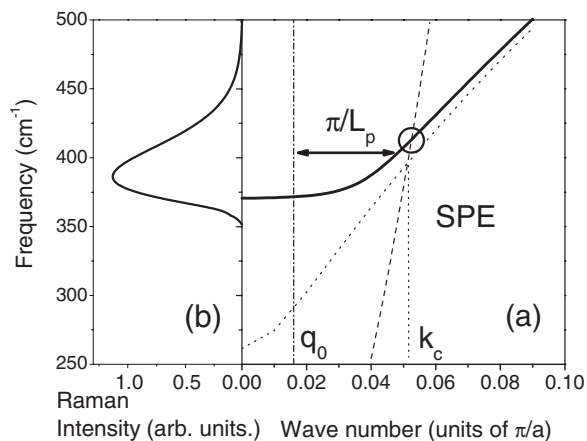
FIG. 5. The full line in panel (a) shows the energy spectrum of the plasmons coupled to the AlAs-like LO phonons calculated in the $Al_{0.11}Ga_{0.89}As$ alloy with the electron concentration $n = 9.0 \times 10^{17}$ cm^{-3}. The dotted line represents the dispersion of the uncoupled plasmons. The dash line shows the spectrum of the single-particle electron excitations. The vertical dash-dotted line indicates the wave number of the light used for excitation. Panel (b) displays the calculated Raman intensity obtained by the fit of the experimental spectrum, as explained in the text.

vibrations. With the increasing doping concentration, the Fermi energy increases and the electrons become delocalized. A typical metallic temperature dependence of the resistivity shown in Fig. 1(b) was found in the alloys with the doping higher than 5×10^{17} cm^{-3}. As a result, the plasmonlike collective excitations emerge. Because of the dispersion of the plasmonlike excitations opposite to the dispersion of the LO phonons, the Raman lines of the collective excitations reveal asymmetries opposite to those of the LO phonons. The typical Raman lines measured in the insulating and metallic $Al_xGa_{1-x}As$ alloys are shown in the corresponding insets of Fig. 4. As illustrated in Fig. 4, a sharp increase of the localization length accompanies the transition from the insulating transport regime to the metallic one. With the further increase of the doping concentration, the localization length of the plasmonlike excitations diminishes due to their interaction with the ionized impurities.[23]

The calculated energy spectra of both the single-particle and collective excitations are depicted in Fig. 5. The collective electron excitations are well defined when the plasma frequency $\omega_p > k v_F + E(k)$, where v_F is the electron velocity at the Fermi surface and $E(k)$ is the energy of the single-particle electron excitations. The wave number cutoff caused by the localization effects (π/L_p) was found in reasonable agreement with the limitation of the wave number of the collective excitations determined by the crossing point of the calculated dispersions of the collective and single-particle excitations (k_c). The value π/k_c, depicted in Fig. 4 as a function of the electron concentration by a dash line, shows that at high enough electron concentration (more than 10^{18} cm^{-3}) the localization of the collective plasmonlike excitations is limited by the effect of the Landau damping. The observed accordance between the expected limitation of the wave number of the collective excitations and the value given by

the experimentally determined localization length L_p demonstrates consistency of the method used to determine the localization length of collective excitations.

Thus, in the metallic $Al_xGa_{1-x}As$ alloys the localization lengths of the single electron were found considerably larger than those of the collective excitations. However, in most of the samples the localization of the collective plasmonlike excitations was limited by the Landau damping and it was not due to the disorder. Therefore, an accurate comparison with the electron localization length was possible only in a narrow interval of the electron concentrations between 5×10^{17} and 1×10^{18} cm^{-3} where the metallic behavior is well pronounced and the condition $\pi/k_c < L_p$ makes the Landau damping irrelevant.

V. LOCALIZATION IN DISORDERED GaAs/Al_xGa_{1-x}As SUPERLATTICES

In order to avoid the effect of the Landau damping, we measured the localization lengths of collective excitations in GaAs/Al_xGa_{1-x}As SLs where the excitation energy of the relevant collective mode falls in the range of the minigap between the minibands. In this case, the disorder determines the localization of both the electrons and their collective excitations and a difference between them is due to the interaction. Raman scattering and the magnetotransport measurements were performed in order to measure the localization of the electron excitations propagated along the growth direction of the SLs. However, a determination of the appropriate localization lengths in the same SL is extremely difficult because the vertical transport measurements can be performed in relatively lowly doped samples, while the plasmon–LO-phonon modes come out in highly doped samples. Therefore, in Ref. 8 the concurrent Raman and magnetotransport measurements were realized in a limited number of samples where we succeeded to measure both the vertical magnetoresistance and Raman scattering. In the present work, a large amount of data obtained for the disordered SLs (some of them from our previous articles) have been analyzed. We demonstrated from all these data the significant increase of the localization of the collective electron excitations with respect to the single electrons.

First of all, we present the data characterizing the electrons in the disordered SLs studied here. The anisotropic properties of the electron systems formed in the disordered SLs are demonstrated in Fig. 6 and 7. The typical anisotropy of the Shubnikov–de Haas oscillations shown in Fig. 6 is due to the anisotropic character of the disorder and the anisotropy of the effective mass. The characteristic time which determines the quantum mechanical broadening of the electron states on the Fermi surface was found to be shorter along the growth direction $(\tau_\perp)$ than in the in-plane direction of the layers $(\tau_\parallel)$. These characteristic times were obtained by the fit of the magnetoresistances calculated according to Ref. 24 to the experimental magnetotransport data. The disagreements between the experimental magnetoresistance traces and the calculated curves at high magnetic fields are caused by the magnetic "freezing" of the impurities.[25]

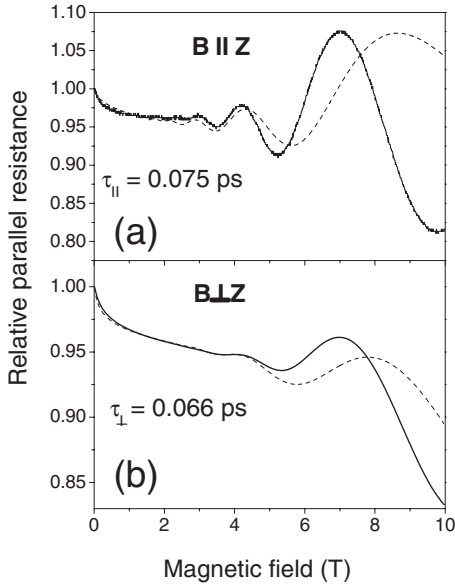The temperature variations of the conductivities depicted in Fig. 7 show the metallic character of the studied SL at low

FIG. 6. Relative high field parallel magnetoresistance of the $(GaAs)_m(Al_{0.3}Ga_{0.6}As)_6$ superlattice with the disorder strength δ_{SL} =0.82 and the electron density $n=2.0\times10^{17}$ cm^{-3} measured at T =1.6 K with different orientations of the magnetic field (full lines) and the calculated magnetoresistances (dash lines).

temperatures. The weak increases of the parallel and vertical conductivities with the temperature observed in the identical SLs grown on semi-insulating and doped substrates, respectively, are assigned to the quantum interference effects being destroyed by the inelastic scattering as the temperature increases. The vertical conductivity [when the current is directed parallel to the growth (disorder) direction] shows a dependence proportional to $T^{0.75}$, while the dependence $T^{1.5}$ fits well the temperature variation of the parallel conductivity (when the current is parallel to the layers); these behaviors are assigned to the electron-electron interaction in dirty metal and to the electron-phonon interaction, respectively.[20]
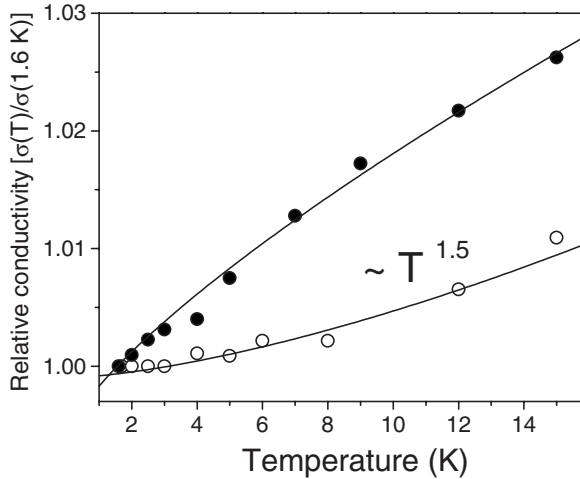

FIG. 7. Temperature dependences of the relative parallel (open circles) and vertical (closed circles) conductivities measured in the $(GaAs)_m(Al_{0.3}Ga_{0.6}As)_6$ superlattices with the disorder strength δ_{SL}=0.4 and the electron density $n=6.5\times10^{17}$ cm^{-3}.
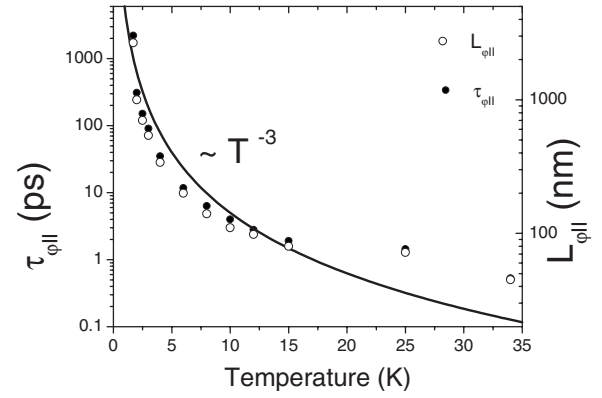

FIG. 8. Temperature dependences of the phase-breaking time ($\tau_{\varphi\parallel}$) and of the coherence length ($L_{\varphi\parallel}$) of the electrons propagated parallel to the layers in the $(GaAs)_m(Al_{0.3}Ga_{0.6}As)_6$ superlattice with the disorder strength δ_{SL}=0.82 and the electron density n =2.0×10^{17} cm^{-3}.

Moreover, the temperature dependences of the phase-breaking time and of the coherence length of the electrons propagated parallel to the layers also reveal the metallic characters: their typical behaviors shown for one of the samples in Fig. 8 follow the T^{-3} dependence, characteristic of the electron-phonon interaction.[20]

Thus, as it follows from the presented magnetotransport data, the electrons in the SLs under investigation exhibit properties of an anisotropic three-dimensional metallic system subject to the anisotropic disorder.

The phase-breaking lengths of the electrons propagated perpendicular to the layers of the disordered SLs associated with the corresponding electron localization lengths are depicted in Fig. 9(a) as a function of the disorder strength. These data exhibit remarkable decrease of the phase-breaking length with the increasing disorder. The bars mark the interval containing the values of the localization lengths obtained for 100 different realizations of 50-period superlattices for each value of the disorder parameter. Good agreement between the calculated and experimental data was obtained without the use of any fitting parameter, and that proves the validity of the experimental method to obtain the localization length in the growth direction.

The localization lengths of the plasmons coupled to the AlAs LO phonons (which reveal mostly the plasmon character) were obtained in the SLs with different disorder strengths by fits of Raman scattering intensities as in Ref. 8, and they are shown in Fig. 9(b). These data also reveal a significant decrease of the localization length of the collective plasmonlike excitations with the increasing disorder. Moreover, in the whole range of the disorder variation we found the localization lengths of the collective excitations to be much smaller than those of the single-particle ones.

It ought to be mentioned that due to the reason given above, the electron localization lengths were obtained in the disordered SL with the doping levels lower than those of the disordered SLs used in Raman experiments to determine the localization lengths of the collective excitations. However, the Raman measurements performed in differently doped SLs with a fixed disorder strength [shown in the inset of Fig.
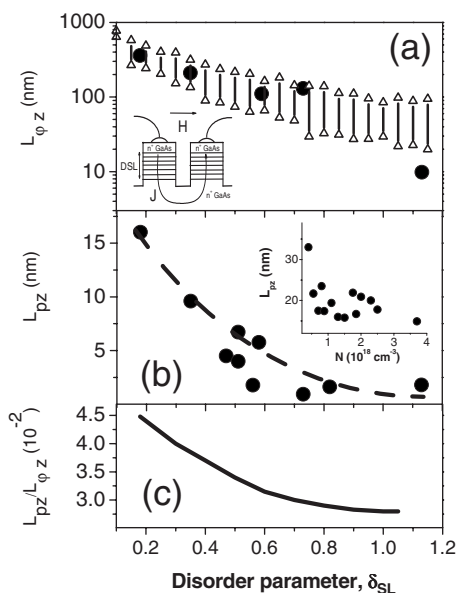
FIG. 9. Localization lengths of (a) the single electrons and (b) their collective excitations measured in the $(GaAs)_m(Al_{0.3}Ga_{0.6}As)_6$ superlattices with different disorder strengths and the fixed electron densities (a) $n=5.0\times10^{17}$ cm^{-3} and (b) $n=1.7\times10^{18}$ cm^{-3}, respectively. Bars in panel (a) mark the interval containing the localization lengths obtained for a hundred different realizations of 50-period disordered superlattices; the inset shows the sample structure used for vertical transport measurements. The inset in panel (b) shows the localization lengths of the collective excitations obtained in the differently doped superlattices with the fixed disorder $\delta_{SL}=0.18$.

9(b)] did not reveal a noteworthy change of the localization length of the collective excitations with the variation of the electron density from 5×10^{17} to 2×10^{18} cm^{-3}. This means a dominant influence of the SL disorder (and not the impurities) on localization of the collective excitations.

VI. CONCLUSIONS

Coherence and localization of electron single-particle and collective excitations were studied in Al$_x$Ga$_{1-x}$As alloys and in the intentionally disordered GaAs/Al$_x$Ga$_{1-x}$As SLs by magnetoresistance and Raman scattering. In the alloys, the disorder was provided by alloy potential fluctuations, while controlled random variation of the well thicknesses introduced during the growth produced the disorder in the SLs. We demonstrated that a variation of the doping level of the alloys resulted in the metal-to-insulator transition confirmed by the temperature behavior of the resistance and by the weak-field magnetoresistance. The localization lengths of collective excitations obtained in the insulating and metallic alloys by the fit of corresponding Raman lines were assigned to the LO phonons and to the coupled plasmon-phonon modes, respectively. They revealed a sharp increase with the increasing electron concentration in the vicinity of the metal-to-insulator transition. Consequently, the metal-to-insulator transition manifested itself in collectivization of the elementary excitations. In most of the alloys, the wave number of the collective plasmonlike excitations was limited by the Landau damping. The calculated wave number cutoffs of these collective excitations were found in good agreement with those determined by the localization lengths obtained in the Raman scattering experiments. The localization lengths of the single-particle and collective excitations were properly compared in the intentionally disordered SLs where, due to the absence of the Landau damping, both of them were limited by the disorder. The quantitatively controlled disorder of these SLs allowed us to make a direct check of the existing localization theories. We found surprisingly good agreement between the experimental and calculated localization lengths of the single-particle excitations without the use of any fitting parameters. In all the disordered SLs considered, the electron localization lengths were found to be significantly larger than those of their collective excitations. The difference between the single-particle and collective excitations is due to the electron polarization which basically determines the properties of the collective excitations. This means that the electron-electron interaction increases the localization.

[1] D. Belitz and T. R. Kirkpatrick, Rev. Mod. Phys. **66**, 261 (1994).

[2] E. Abrahams, S. V. Kravchenko, and M. P. Sarachik, Rev. Mod. Phys. **73**, 251 (2001).

[3] G. Zala, B. N. Narozhny, and I. L. Aleiner, Phys. Rev. B **64**, 214204 (2001).

[4] V. M. Pudalov, M. E. Gershenson, H. Kojima, G. Brunthaler, A. Prinz, and G. Bauer, Phys. Rev. Lett. **91**, 126403 (2003).

[5] T. Vojta, F. Epperlein, and M. Schreiber, Phys. Rev. Lett. **81**, 4212 (1998).

[6] K. Byczuk, W. Hofstetter, and D. Vollhardt, Phys. Rev. Lett. **94**, 056404 (2005).

[7] A. Lewalle, M. Pepper, C. J. B. Ford, E. H. Hwang, S. Das Sarma, D. J. Paul, and G. Redmond, Phys. Rev. B **66**, 075324 (2002).

[8] Yu. A. Pusep, M. B. Ribeiro, V. E. Carrasco, G. Zanelatto, and J. C. Galzerani, Phys. Rev. Lett. **94**, 136407 (2005).

[9] L. Esaki and R. Tsu, IBM J. Res. Dev. **14**, 61 (1970).

[10] A. Chomette, B. Deveaud, A. Regreny, and G. Bastard, Phys. Rev. Lett. **57**, 1464 (1986).

[11] E. Tuncel and L. Pavesi, Philos. Mag. B **65**, 213 (1992).

[12] W. Szott, C. Jedrzejek, and W. P. Kirk, Phys. Rev. B **40**, 1790 (1989).

[13] A. Kawabata, J. Phys. Soc. Jpn. **40**, 628 (1980).

[14] A. Cassam-Chenaï and D. Mailly, Phys. Rev. B **52**, 1984 (1995).

[15] R. Merlin, in *Light Scattering in Solids V*, edited by M. Cardona and G. Güntherodt (Springer-Verlag, Heidelberg, 1989).

[16] Yu. A. Pusep, W. Fortunato, P. P. Gonzalez-Borrero, A. I. Toropov, and J. C. Galzerani, Phys. Rev. B **63**, 115311 (2001).

[17] A. Pinczuk, G. Abstreiter, R. Trommer, and M. Cardona, Solid State Commun. **21**, 959 (1977).

[18] J. Singh, *Physics of Semiconductors and Their Heterostructures* (McGraw-Hill, New York, 1993).

[19] N. F. Mott, J. Non-Cryst. Solids **1**, 1 (1968).

[20] P. A. Lee and T. V. Ramakrishnan, Rev. Mod. Phys. **57**, 287 (1985).

[21] Yu. A. Pusep, H. Arakaki, and C. A. de Souza, Phys. Rev. B **68**, 205321 (2003).

[22] D. Pines and P. Nozieres, *The Theory of Quantum Liquids* (Benjamin, New York, 1966), Vol. 1.

[23] Yu. A. Pusep, S. S. Sokolov, W. Fortunato, J. C. Galzerani, and J. R. Leite, J. Phys.: Condens. Matter **13**, 10165 (2001).

[24] A. E. Stephens, D. G. Seiler, J. R. Sybert, and H. J. Mackey, Phys. Rev. B **11**, 4999 (1975).

[25] B. M. Askerov, *Electron Transport Phenomena in Semiconductors* (World Scientific, Singapore, 1994).